JOURNAL OF MOLECULAR SPECTROSCOPY 58, 283–300 (1975)

A New Electronic Band System of PbO

R. C. OLDENBORG,[1] C. R. DICKSON, AND R. N. ZARE

Department of Chemistry, Columbia University, New York, New York 10027

The chemiluminescence spectrum of atomic Pb reacting with O_3 under single-collision conditions includes a series of 55 bands in the regions 450–850 nm. A vibrational analysis is obtained which shows emission is to the ground state of PbO from excited electronic states not previously analyzed. Forty-nine of the bands are assigned to the $a(1)$–$X(0^+)$ transition and the remaining six are tentatively identified as the forbidden $b(0^-)$–$X(0^+)$ transition. Both the a and b states are believed to be Hund's case (c) components of the $^3\Sigma^+$ states arising from the configuration $\sigma^2\pi^3\pi^*$. The vibrational parameters of the a state are $\nu_e = 16\,029 \pm 8$, $\omega_e' = 478.7 \pm 1.9$, and $\omega_e x_e' = 2.292 \pm 0.128$ cm^{-1}, where the uncertainties represent two standard deviations of the least-squares fit. Emission is also observed from the PbO B state produced in the reaction of metastable Pb atoms with O_3. Using pulsed laser excitation, an attempt is made to determine radiative lifetimes. We find for the PbO $A(0^+)$ state $\tau = 3.74 \pm 0.3$ μsec, and for the PbO $B(1)$ state $\tau = 2.58 \pm 0.3$ μsec, while for the $a(1)$ state τ is estimated to be greater than 10 μsec. From the vibrational analysis, energy conservation arguments place a lower limits to the ground state dissociation energy of $D_0^0(\text{PbO}) \geq 3.74 \pm 0.03$ eV (86.2 ± 0.7 kcal/mole). For the Pb + O_3 reaction we find less than 1% of the products are PbO* molecules that emit in the visible. Correlations are made with the low-lying states of other Group IV chalconides based on the assignment of the PbO $a\,^3\Sigma^+(1)$ state and the correspondence between the low-lying triplet states of PbO and CO.

I. INTRODUCTION

Radiative intercombination bands of the Group IV diatomic oxides, from CO to PbO, have been the focus of many previous spectroscopic studies (*1*). The lowest-lying molecular states arise from the molecular orbital configurations

$$\sigma^2\pi^4, \qquad {}^1\Sigma^+, \tag{1}$$

$$\sigma^2\pi^3\pi^*, \qquad {}^3\Sigma^+, {}^3\Delta, {}^3\Sigma^-, {}^1\Sigma^-, {}^1\Delta, {}^1\Sigma^+, \tag{2}$$

$$\sigma\pi^4\pi^*, \qquad {}^3\Pi_r, {}^1\Pi, \tag{3}$$

where the states are listed in order of increasing energy as predicted by simple molecular orbital theory (*2*). Because the σ and π molecular orbitals are nearly isoenergetic for these compounds, the $\sigma^2\pi^3\pi^*$ and $\sigma\pi^4\pi^*$ configurations have comparable energies, causing the molecular states arising from these configurations to be interleaved. Thus the longest wavelength transitions of the Group IV monoxides are expected to be the intercombination bands $^3\Pi_r$–$X\,^1\Sigma^+$ and $^3\Sigma^+$–$X\,^1\Sigma^+$. For CO these are recognized as the Cameron and the Hopfield–Birge band systems, respectively.

[1] Present address: Group L-8, Los Alamos Scientific Laboratory, Los Alamos, N. M. 87544.

Although the identification and ordering of the low-lying electronic states of CO are well known (*3*), some confusion arises for the heavier Group IV monoxides. The origin of this difficulty can be traced to two problems: (i) the relative ordering of the $\sigma^2\pi^3\pi^*$ and $\sigma\pi^4\pi^*$ configurations; and (ii) the tendency for Hund's coupling case (*c*) to become a more appropriate description with increasing spin–orbit splitting of the Group IV elements. Whereas the ^3P ground state of the carbon atom is split into three multiplets, $^3P_0$, $^3P_1$, and $^3P_2$, separated by only 43 cm^{-1}, the ^3P multiplets of lead are separated by 10 650 cm^{-1}. In going from carbon to lead, the increasing spin–orbit interaction causes the intensity of the intercombination bands to grow by spoiling the spin quantum number. Consequently, the identification of the low-lying electronic states of the heavier diatomic Group IV chalconides (oxides, sulfides, selenides, and tellurides) and their correlation with the electronic configuration from which they arise has proved puzzling.

We report here the observation and analysis of a new intercombination band system for the PbO molecule. On the basis of this work, we show that the $^3\Sigma^+$ state of the $\sigma^2\pi^3\pi^*$ configuration falls below the $^3\Pi_r$ state of the $\sigma\pi^4\pi^*$ configuration in going from CO to PbO. This permits us to extend the systemization of the low-lying electronic states of the Group IV chalconides, started by Barrow (*4*).

The earliest spectroscopic investigators of PbO were Lamprecht (*5*) and Eder and Valenta (*6*), who observed band spectra by introducing lead chloride in a gas flame. Grebe and Konen (*7*) excited similar bands using a carbon arc containing lead chloride. Confirmation of PbO as the emitter was first obtained by Bloomenthal (*8*) from the isotope shift resulting when the chloride of ordinary lead and lead derived from the radioactive decay of uranium were introduced into a carbon arc. Subsequently, high-resolution absorption studies of PbO have been carried out by Shawhan and Morgan (*9*), Howell (*10*), Vago and Barrow (*11*), and Barrow, Deutsch, and Travis (*12*). These, together with the high-resolution emission studies of Christy and Bloomenthal (*13*), and Ram, Singh, and Upadhya (*14*), have shown that there are at least six band systems of PbO above 200 nm, all of which terminate on the ground state. In the visible portion of the spectrum the most prominent bands are the $A(0^+)$ at T_{00} = 19 725 cm^{-1} and the $B(1)$ at T_{00} = 22 175 cm^{-1}, both of which have been rotationally analyzed. We decided to apply the technique of beam-gas chemiluminescence (*15*) and laser-induced fluorescence (*16*) to the study of the low-lying excited state of PbO. We began this study in hopes of gaining better characterizations of these states, and those of the other Group IV chalconides.

II. EXPERIMENTAL DETAILS

The spectroscopic source, consisting of an atomic beam traversing a chamber filled at low pressure with scattering gas, is fairly unusual in that the excited-state species produced by chemical reaction undergo virtually no collisions before radiating. Consequently, the appearance of the collisionally-unrelaxed chemiluminescence spectrum may be markedly different from that obtained in an arc or a flame.

The beam-gas apparatus, called LABSTAR, has been described previously (*15*, *17*). A new beam source, constructed from a modified Astro Industries furnace, has been incorporated into the apparatus (*18*). In this chamber a resistively heated tube surrounds a crucible containing high-purity lead powder (99.9999%, Alfa-Ventron Corp.), gen-

erating an effusive lead beam. Both the oven heater and crucible are constructed from graphite because of its apparent inertness to molten lead. Oven temperatures, measured with a W 5% Re/W 26% Re thermocouple, are typically 1100 K corresponding to a Pb vapor pressure of 0.1 Torr (*19*), The thermocouple outputs are fed into an Electromax C.A.T. controller (Leeds and Northrup) that regulates the heater current with a pair of silicon-controlled rectifiers (SCR's) which alternately fire at 60 Hz.

The lead beam passes through several collimating heat shields and enters a second chamber, called the scattering chamber, containing ozone at typically 10^{-4} Torr. The pressure measurement is only approximate and represents the uncorrected reading of a vacuum ionization gauge, located 40 cm from the reaction zone. The ozone is generated with a Welsbach ozonizer and is adsorbed onto silica gel cooled to the temperature of a dry ice and acetone slush. The chemiluminescence passes through a port window in the side of the scattering chamber and is imaged (1:1) by a quartz lens on the entrance slits of a 1 m Interactive Technology scanning spectrometer. A cooled photomultiplier (RCA C31034, gallium arsenide 128 photocathode) is attached to the exit slits of the spectrometer. The entire optical detection system is calibrated using an Optronic Laboratories Model 245C standard lamp to provide absolute photon yields (*20*).

The LABSTAR apparatus has also been modified to permit laser-induced fluorescence studies. A 100 kW pulsed (AVCO) nitrogen laser is used to pump a noncirculating dye solution. The dye laser cavity is formed by a 50% reflecting output mirror and a 600 groove/mm diffraction grating (Bausch and Lomb) operated near its blaze angle. An intracavity 20 power telescope expands the laser beam to fill the grating and narrows its bandwidth to approximately 0.1 nm. The dyes 7-diethylamino-4-methylcoumarin, coumarin 102, and fluorescein disodium salt ($\sim 5 \times 10^{-3}$ *M* solution in ethanol) cover the wavelength ranges of interest, 437–490, 460–510, and 530–570 nm, respectively. The dye laser pulsewidth is typically 5 nsec at 20 pps and each pulse contains several microjoules of radiant energy.

The laser beam enters and exits the LABSTAR scattering chamber perpendicular to the metal beam via two 50 cm light baffles. The fluorescence is observed perpendicular to both the metal and laser beams with a photomultiplier tube (RCA 7265, S-20 photocathode). Signals are processed using gated detection electronics. Two different boxcar integrators are used for different aspects of this work. A PAR model 162 with model 164 plug-in is used to measure the radiative decay of the fluorescence signal. The boxcar integrator and nitrogen laser are both triggered from a pulse generator and the opening of the boxcar gate is scanned in time with a gate width of 200 nsec, corresponding to less than 10% of the measured lifetime. A Keithley model 881 linear gate and model 882 scan delay generator are used to obtain excitation spectra. Here the gate is opened with about a 20 nsec delay (to avoid scattered laser light) and has a width of 2 μsec.

We attempted to observe PbO fluorescence by exciting the ground state PbO products formed in a chemical reaction of Pb with various oxidizer gases. However, the low concentration of PbO obtained by this means combined with the long radiative life times of the PbO excited states prevented this measurement using present laser power levels. Instead, we chose to generate a beam of PbO by heating PbO powder (Alfa-Ventron Corp., 99.9% purity) in an alumina oven to a temperature range of 1100–1200 K. Graphite ovens cannot be used in this case since they readily reduce the PbO to metallic lead.

Table 1. Measured PbO bandhead positions and vibrational assignments.

bandhead position (cm^{-1})	relative intensity	bandhead assignment (v',v'')	obs.–calc. (cm^{-1})	remarks
21712	1	(13,0)	–0.93	a
21643	1	[12,0]	—	a, b, e
21407	1	(14,1)	–4.99	a
21289	1	(12,0)	–4.86	a, b, d
21200	3	[11,0]	—	e
20993	1	(13,1)	–4.50	a
20861	3	(11,0)	–9.19	a
20786	1	[10,0]	—	e
20573	1	(12,1)	–5.42	
20435	5	(10,0)	–6.94	
20354	1	[9,0]	—	e
20149	2	(11,1)	–5.75	
20008	8	(9,0)	–1.11	
19923	1	[8,0]	—	e
19726	1	(10,1)	–0.50	
19572	9	(8,0)	0.30	
19453	1	(11,2)	6.15	
19130	10	(7,0)	0.30	
19014	1	(10,2)	–4.60	
18754	1	(11,3)	7.53	
18679	10	(6,0)	–4.11	
18586	2	(9,2)	0.23	
18410	1	(7,1)	–4.26	a
18323	1	(10,3)	4.78	a
18236	7	(5,0)	4.06	
18157	2	(8,2)	8.65	
17969	3	(6,1)	1.33	
17778	6	(4,0)	1.81	
17710	1	(7,2)	3.65	
17521	6	(5,1)	4.50	
17319	3	(3,0)	3.14	
17200	1	[2,0]	—	a, e
17060	7	(4,1)	–0.75	b
16846	1	(2,0)	–4.93	
16599	7	(3,1)	–1.42	b, c
16352	1	(4,2)	–0.85	
16141	4	(2,1)	5.50	a

III. CHEMILUMINESCENT SPECTRUM

Figure 1 shows the lead plus ozone chemiluminescent spectrum under low resolution (0.5 nm). There are two distinct molecular features, both of which are attributable to the PbO emitter. The relative intensities of these features change during the length of a run (2–3 hr) and with experimental conditions. Between 370 and 450 nm is a band system believed to be the PbO $B \rightarrow X$, but which is too poorly resolved to be spectrally analyzed. Between 450 and 850 nm is a series of sharp red-degraded bandheads which are vibrationally analyzed below. Although the bandheads are clearly separated, rotational structure is only apparent at high rotational levels because of the low resolution employed.

A total of 55 bandhead positions have been measured for the longer wavelength molecular feature and are listed in Table I. A comparison of the bandhead positions with those reported in the literature shows that only some of the weaker bands could possibly belong to the A–X or B–X systems. However, seven of the stronger bandheads, indicated in Table I, correspond to bandheads previously observed by Lamprecht (*5*), Eder and Valenta (*6*), or Bloomenthal (*8*), but reported as unidentified.

The positions of 49 bandheads, including those we originally considered as possibly belonging to the A–X and B–X systems, can be fitted into a Deslandres table, yielding

Table 1. (continued, p. 2)

bandhead position (cm^{-1})	relative intensity	bandhead assignment (v',v'')	obs.–calc. (cm^{-1})	remarks
15893	4	(3,2)	0.49	b, c
15645	2	(4,3)	–7.47	a
15422	6	(2,2)	–5.59	b, d
15199	1	(3,3)	6.86	
14961	4	(1,2)	2.91	b, d
14724	3	(2,3)	–3.21	
14508	1	(3,4)	8,71	
14251	3	(1,3)	–6.71	
14044	1	(2,4)	9.63	a
13818	1	(3,5)	4.02	
13780	2	(0,3)	–3.63	
13561	1	(1,4)	–3.87	
13089	1	(0,4)	–1.78	
12933	1	(4,7)	6.71	a
12672	1	(2,6)	0.72	
12400	1	(0,5)	–5.47	
12004	1	(2,7)	2.97	a
11720	1	(0,6)	–7.69	a

[a] Position less certain due to low intensity or overlapping bandheads.

[b] Observed also by Eder and Valenta but reported as unidentified (8).

[c] Observed also by Lamprecht but reported as unidentified (8).

[d] Observed also by Bloomenthal but reported as unidentified (8).

[e] Tentative assignment, b–X band system, see text.

vibrational quantum number assignments. Table II presents the Deslandres table where the numbers indicate the relative band intensities, uncorrected for detector response. Note how the intensity pattern follows the expected Franck–Condon distribution.

Assuming that the head is close to the band origin, the formula that gives the position of the bandheads is

$$\nu = \nu_e + \omega_e'(v' + \tfrac{1}{2}) - \omega_e x_e'(v' + \tfrac{1}{2})^2 - \omega_e''(v'' + \tfrac{1}{2}) + \omega_e x_e''(v'' + \tfrac{1}{2})^2, \qquad (4)$$

where the symbols have their traditional meanings (*21*). The positions of the 49 heads were fit to Eq. (4) by the method of least squares. Figure 2 shows a portion of the PbO chemiluminescent spectrum taken under the same conditions as Fig. 1 but with a slower scan speed. The (7, 0) and (8, 0) bands are clearly apparent while the (10, 2) and (11, 2)

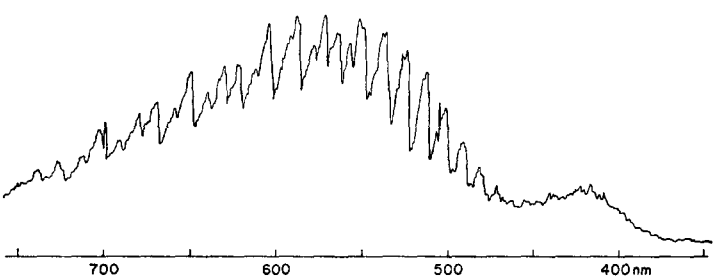

FIG. 1. The chemiluminescent spectrum of PbO from the reaction of atomic Pb with O_3 (0.5 nm resolution).

TABLE II

DESLANDRES TABLE OF PbO a–X BAND INTENSITIES

v′ \ v″	0	1	2	3	4	5	6	7
0				2	1	1	1	
1			4	3	1			
2	1	4	6	3	1		1	1
3	3	7	4	1	1	1		
4	6	7	1	2				1
5	7	6						
6	10	3						
7	10	1	1					
8	9		2					
9	8		2					
10	5	1	1	1				
11	3	2	1	1				
12	1	1						
13	1	1						
14		1						

bands are much less pronounced. Since the positions of the more intense bandheads can be more accurately measured, weights were assigned proportional to the relative intensities in the fitting procedure. The derived constants together with twice their standard error estimates, corresponding to a 90% confidence limit, are listed in Table III. In Table I we also present the differences between the observed and calculated positions. All calculated positions agree to within 10 cm^{-1} of the experimental values.

Table III also lists vibrational constants and term values derived by Bloomenthal (*8*) from a bandhead analysis of the PbO A–X and B–X bands observed in emission. The values of ω_e'' and $\omega_e x_e''$ agree with those from our analysis to well within one standard error. This proves that the emitter is the diatomic molecule PbO and that the emission terminates on the ground state. Although the values of ω_e' and $\omega_e x_e'$ are similar to those of the A and B states, we are clearly observing a new electronic state that lies below the A state, hereafter called the a state.

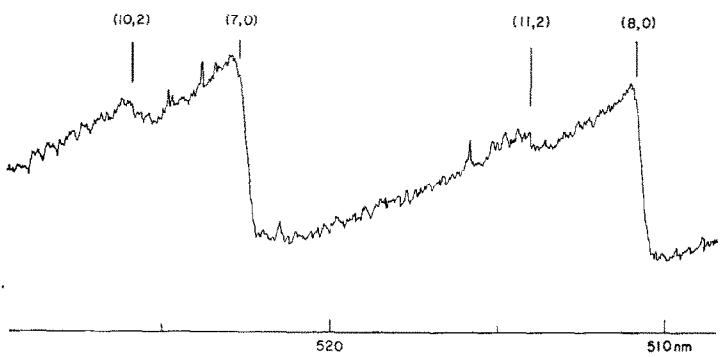

FIG. 2. Enlargement of a small portion of the chemiluminescent spectrum of PbO showing several a–X bandheads (0.5 nm resolution).

TABLE III

PbO VIBRATIONAL CONSTANTS (cm^{-1})

state	ν_e	ω_e	$\omega_e x_e$	
X	0	722·9 ± 2·8	3·766 ± 0·400	This Work
a	16029 ± 8	478·7 ± 1·9	2·292 ± 0·128	This Work
X	0	722·3	3·73	Ref. (8)
A	19863·3	451·7	3·33	Ref. (8)
B	22289·8	496·3	2·33	Ref. (8)

Six bandheads remain that do not belong to any analyzed PbO band system including the new a–X system. Although a reliable analysis cannot be accomplished with so little data, certain conclusions can be inferred. The six bands appear to belong to a single v' progression with spacings comparable to the separation between vibrational levels of the a state. This strongly suggests that the bands belong to another electronic state, hereafter called the b state, lying near the a state and having approximately the same shape, and hence similar vibrational constants. With this assumption, we can assign the v' numbering to ± 1 unit. We further speculate that the six bands might belong to the $(v', 0)$ progression in the b state, since the corresponding $(v', 0)$ progression in the a state is the most intense. This would place the b state at 350 ± 430 cm^{-1} above the a state, where the error estimate reflects the uncertainty in the v' quantum number assignment. However, a comparison of the intensities of the $(v', 0)$ b–X bands with the corresponding $(v', 0)$ a–X bands shows that the emission from the b state is very weak but does not follow the distribution predicted simply from the Franck–Condon principle. This may imply that the above reasoning about the vibrational numbering is incorrect or that the intensity is derived largely from perturbations.

IV. RADIATIVE LIFETIMES

Some information on the radiative lifetimes of the a and b states can be deduced from the intensity of the chemiluminescence. Figure 3 is a photograph of the reaction zone showing the chemiluminescence, which assumes the shape of the lead beam. The lead beam is narrow and well defined (see Experimental section). If the lifetime of the PbO emitter is long, excited molecules travel outside the beam before radiating, and the chemiluminescence appears diffuse. This diffuseness is apparent in the Pb + O_3 chemiluminescence (see Fig. 3) and permits us to estimate that the radiative lifetime of the PbO a state must be greater than several microseconds.

Emission from the PbO b state is much weaker than that of the a state (see Table I). This implies that either the b state is not populated to the same extent as the a state by the Pb + O_3 reaction, or the b–X transition strength is much smaller than the a–X. We favor the second interpretation since the a and b states are so close in energy and

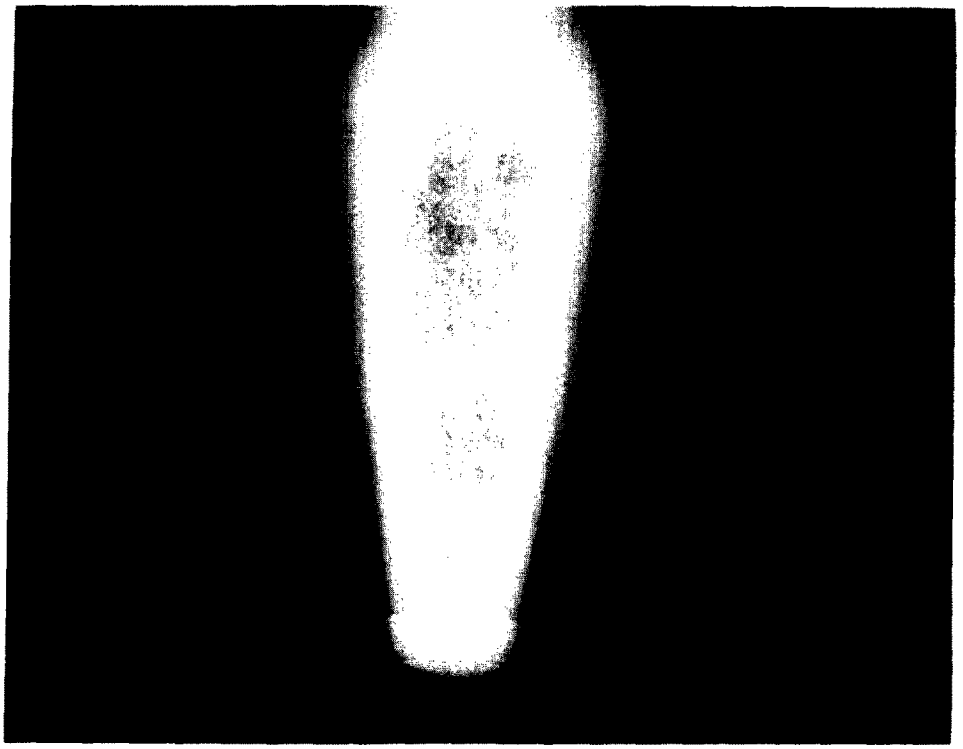

FIG. 3. Photograph of the PbO chemiluminescence in the scattering chamber. The metal beam vertically enters the chamber through a 1 cm hole.

since there are no apparent symmetry restrictions on the reaction. Thus we believe that the radiative lifetime of the *b* state is much longer than that of the *a* state.

The above arguments are indirect. In order to obtain quantitative information on the radiative lifetimes of the PbO *a* and *b* states, we attempted to observe the direct decay of their fluorescence signal following excitation of a PbO beam by a pulsed tunable dye laser (*22*). Unfortunately, fluorescence signals proved to be too weak to permit a life-

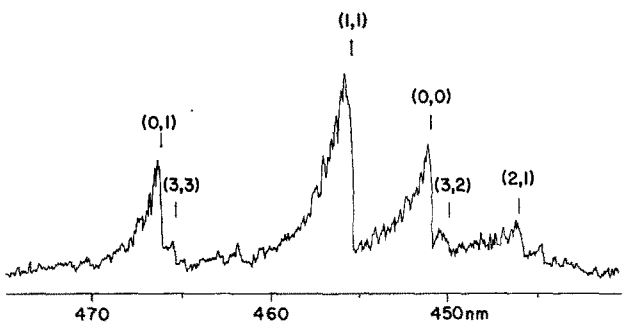

FIG. 4. Portion of the fluorescence excitation spectrum of a PbO beam showing bandheads of the PbO *B*–*X* system (0.1 nm resolution).

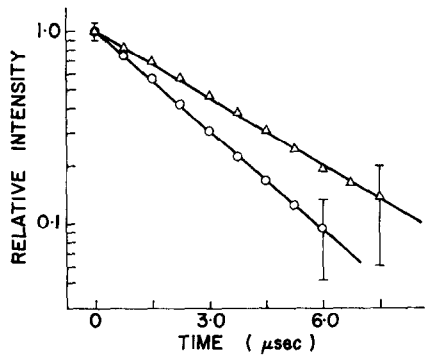

FIG. 5. Semilograthmic plot of the relative fluorescence intensity of PbO vs time. The circles represent data for the A state ($v' = 2$ level) and the triangles represent the combined data for the B state ($v' = 0$ and 1 levels). The circles and triangles are the average values for approximately 100 laser shots and the error bars indicate the scatter.

time determination when the laser is tuned to the a–X and b–X absorption bands, but we have obtained the radiative lifetimes of the PbO A and B states.

Figure 4 shows a typical PbO fluorescence excitation spectrum when a thermal beam of PbO is excited in the spectral range 445–470 nm. The bandheads of the PbO B–X system are readily identified. Similarly, the bandheads of the PbO A–X system are also found when the laser is scanned in the spectral range 460–510 nm.

Figure 5 shows a semilogarithmic plot of the fluorescence intensity versus time for both the PbO A and B states. The PbO A state is excited by pumping of the (2, 0) band, while the data for the PbO B state represent excitation of both the (0, 1) and (1, 1) bands, since fits to the individual bands are identical to within experimental error. Each point in Fig. 5 represents the average of roughly 100 laser shots and the error bars indicate the scatter. We find

$$\text{PbO } A\ v' = 2, \qquad \tau = 3.75 \pm 0.3\ \mu\text{sec}; \tag{5}$$

$$\text{PbO } B\ v' = 0, 1, \qquad \tau = 2.58 \pm 0.3\ \mu\text{sec}. \tag{6}$$

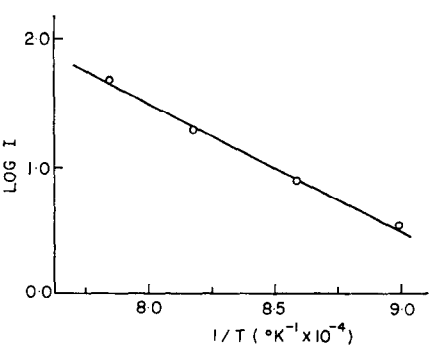

FIG. 6. Plot of the logarithm of the chemiluminescent intensity for the (6, 0) band of the PbO a–X system vs the reciprocal of the lead oven temperature.

The uncertainties in the lifetimes are primarily caused by statistical noise in the small number of photons collected per laser shot. Note that the lifetimes represent all radiative loss processes, including possible transitions to states other than the ground state. Because these relatively long lifetimes are measured at ultralow pressures under collision-free conditions, these values should not be impaired by systematic errors resulting from radiation trapping, quenching, and energy transfer.

Although there appears to be no previous measurement of the radiative lifetime of the PbO A state, Johnson (*23*) reports in his thesis that the radiative lifetime of the PbO B state is 1.5 ± 0.3 μsec. The PbO is generated by reacting Pb atoms in a N_2 carrier gas with discharged O_2. Direct lifetime measurements with a tunable dye laser were made in the pressure range 1.8–20 Torr. Surprisingly, no difference could be detected in the measured lifetime as a function of pressure, and consequently, no Stern–Volmer plots were made. We believe that quenching by the N_2 carrier gas may nevertheless account for the shorter lifetime value reported.

A very weak fluorescence signal, at least an order of magnitude weaker than the PbO A or B state fluorescence, is detected in the spectral region, 530–570 nm, of the a–X absorption bands, but the intensity is not sufficient to measure a lifetime directly. It should be appreciated that the intensity of the fluorescence signal per unit time interval decreases approximately as the square of the lifetime since the excitation is weaker and the emission per unit time interval is reduced. We estimate from the strength of the fluorescence that the a state lifetime must be 10 μsec or longer.

V. REACTION KINETICS

The PbO a state is populated by the bimolecular reaction between ground state lead atoms and ozone:

$$Pb(^3P_0) + O_3 \rightarrow PbO^*(a\,^3\Sigma^+) + O_2. \tag{7}$$

The order of the reaction with respect to the metallic species is determined by studying the chemiluminescence intensity as a function of oven temperature. Figure 6 shows a plot of the logarithm of the intensity versus the reciprocal of the oven temperature. The data points are satisfactorily fit by a straight line whose slope represents the sum of the heat of vaporization of the participating metallic species and the activation energy of the reaction (*15*). The value we obtain, 46.0 ± 0.7 kcal/mole, closely approximates the heat of vaporization of atomic lead (*19*). Thus, we conclude that (i) the chemiluminescence is first order in ground state Pb, with no dependence on other beam components such as Pb_2, and (ii) the activation energy of reaction (7) is small.

The reaction order with respect to ozone is determined by fitting the chemiluminescent intensity as a function of ozone pressure p to the expression $p^n \exp(-\alpha p)$, where n is the reaction order and α is the attenuation factor. The linearity of the chemiluminescent intensity with ozone pressure at low pressures ($<10^{-4}$ Torr) demonstrates that the reaction is first order in ozone.

The factor $\exp(-\alpha p)$ corrects for the attenuation of the metal beam which occurs prior to its crossing the observation zone of the spectrometer. At higher pressures, this factor becomes significant and permits a determination of α. The value of α together with the attenuation path length yields a phenomenological cross section of 135 ± 30 Å^2 for the removal of metal atoms from the beam. Since elastic scattering cross sections

are much smaller, we attribute this cross section primarily to all reactive processes. However, the absolute photon yield measurements indicate that approximately only one reactive collision in several hundred yields a PbO a state product. Hence, the vast majority of the Pb + O_3 reactions yield "dark" products, and we are studying the chemiluminescence from a rather rare bimolecular collision process, made possible by the sensitivity of this technique.

It cannot be assumed that the other molecular feature in the chemiluminescent spectrum, the PbO B–X band system, is also produced in reaction (7), since the relative intensities of these two distinct features change with experiment conditions. Therefore, the dependence on reaction conditions for this feature was also studied. The chemiluminescent intensity is first order in ozone pressure but varies strangely with changes in oven temperature. For example, over certain temperature ranges, the intensity actually decreases with increasing oven temperature. It was found that the PbO $B \rightarrow X$ chemiluminescence signal has a large AC component that closely follows the 60 Hz output of the SCR's in the oven heater circuit. The thermal time constant of the oven is much too long for the temperature to be following rapid current fluctuations, and no such AC component is found in the $a \rightarrow X$ chemiluminescence. We conclude that a minor discharge must be occurring near the oven, exciting some of the Pb atoms to the metastable $^3P_1$ or $^3P_2$ levels, and that it is the bimolecular reaction of these metastables with O_3 which is responsible for the PbO $B \rightarrow X$ chemiluminescence feature. This reaction does not appear to produce significant amounts of the PbO a state, although this process is energetically feasible. We have no explanation at present for this apparent reaction preference.

VI. DISSOCIATION ENERGY

Golomb and Best (*24*) report that sunlight-induced PbO fluorescence is seen when tetraethyl lead is released in the upper atmosphere. The persistence for more than 100 sec of the PbO fluorescence indicates that PbO is not readily reduced by O, i.e., PbO + O $\not\rightarrow$ Pb + O_2. This observation can be explained by assuming that the PbO + O reaction is slow either on thermodynamic or kinetic grounds. The former possibility has stimulated a reinvestigation of the value of D_0^0(PbO).

The most reliable value of the PbO ground state dissociation energy has been provided by Drowart, Colin, and Exsteen (*25*) through the mass spectrometric study of the vaporization of lead monoxide. They find $D_0^0(\mathrm{PbO}) = 3.83 \pm 0.05$ eV (88.4 ± 1.4 kcal/mole). By examining the spectroscopic data for the PbO E state and assuming that its dissociation products correlate with $\mathrm{Pb}(^3P_1) + \mathrm{O}(^3P_1)$, they also place a lower bound of $D_0^0(\mathrm{PbO}) \geq 3.87$ eV.

It is possible to apply energy conservation arguments and derive from the collisionally unrelaxed chemiluminescence spectrum an independent lower bound on D_0^0(PbO) (*26*). For reaction (7) we obtain the inequality

$$D_0^0(\mathrm{PbO}) \geq D_0^0(\mathrm{O_2\text{–}O}) + E_{\mathrm{int}}(\mathrm{PbO}) - E_{\mathrm{int}}(\mathrm{Pb}) - E_{\mathrm{int}}(\mathrm{O_3}) - E_{\mathrm{trans}}{}', \qquad (8)$$

where E_{int} is the internal energy and $E_{\mathrm{trans}}{}'$ is the initial relative translational energy, measured in the center-of-mass reference frame. The inequality is the result of having neglected the internal energy of the O_2 product and the final relative translational energy of the products.

The dissociation energy of O_3 is taken to be $D_0^0(O_2\text{–}O) = 1.05 \pm 0.02$ eV (*26*). The value of $E_{int}(PbO)$ is calculated to be 2.788 ± 0.012 eV, using the highest vibrational level observed in the PbO a state, $v' = 14$. Here the uncertainty represents three standard deviations of our least-squares fit. The value of $E_{int}(O_3)$ is calculated to be 0.039 eV at $T = 300$ K, where we consider only the average rotational energy ($\frac{3}{2}RT$) and regard the vibrational excitation as negligible. We estimate $E_{int}(Pb) = 0$ since the multiplet splitting of Pb ^3P is so large compared to thermal energies. Finally, the initial relative translational energy is estimated (*22*) to be $E_{trans}^i = 0.059$ eV, where the temperature of the Pb is taken as 1106 K.

With these values, Eq. (3) yields

$$D_0^0(PbO) \geq 3.740 \pm 0.032 \text{ eV}. \tag{9}$$

This is in good agreement with the value found by Drowart *et al.*, which demonstrates once again that dissociation energies derived from chemiluminescence studies under single-collision conditions are reliable when a vibrational analysis can be performed.

The ground state dissociation energy of O_2 is $D_0^0(O_2) = 5.12$ eV. Thus the PbO + O $\rightarrow$ Pb + O_2 reaction is exothermic and cannot be slow on thermodynamic grounds. Moreover, this reaction obeys spin conservation, where PbO($^1\Sigma$) + O(^3P) reacts on a triplet surface which correlates with Pb(^3P) + $O_2(^3\Sigma_g^-)$. However, the PbO–O intermediate must also be a triplet, which lies above the singlet ground state of PbO_2. This suggests that an activation energy causes the apparent slowness of the PbO + O reaction.

VII. DISCUSSION

While this spectroscopic study is primarily devoted to the previously undetected $a(1)$–$X(0^+)$ intercombination band system of PbO, the identification of this new upper state permits us to extend the systemization of the low-lying electronic states of the Group IV chalconides. The longest wavelength intercombination bands of CO are the $a\ ^3\Pi_r$–$X\ ^1\Sigma^+$ Cameron bands and the $a'\ ^3\Sigma^+$–$X\ ^1\Sigma^+$ Birge–Hopfield bands, where the $a'\ ^3\Sigma^+$ state at 6.86 eV is located above the $a\ ^3\Pi_r$ state at 6.01 eV (*3*). This ordering of the $^3\Sigma^+$ and $^3\Pi_r$ states is subject to change because these states arise from two different molecular orbital configurations, $\sigma^2\pi^3\pi^*$ and $\sigma\pi^4\pi^*$, which are nearly isoenergetic. It is interesting to consider this ordering for the isoelectronic series BF, CO, and N_2. For BF, having the electronic structure B^-F^+ (*27*), the $a\ ^3\Pi$ state lies about 4 eV below the $b\ ^3\Sigma^+$ state; for CO, having the electronic structure $C^{\delta-}O^{\delta+}$, this separation is reduced to 0.85 eV; whereas in N_2 the order is reversed, the $A\ ^3\Sigma_u^+$ state lying about 1 eV below the $B\ ^3\Pi_g$ state (*21*). We note an apparent correlation between the ordering of the π and σ molecular orbitals and the sign of the dipole moment, as might be expected considering that these orbitals are localized on different atoms (*28*). The next member of the Group IV oxides, silicon monoxide, has an electronic structure of the form Si^+O^- (*29*). Since the sign of the dipole moment is reversed from carbon monoxide, it is not surprising to find that the experimental evidence places the $^3\Sigma^+$ state 0.05 eV below the $^3\Pi_r$ state at 4.20 eV (*30, 31*). As we go to the oxides of the heavier Group IV elements, the energy positions of both states fall in magnitude with the $^3\Sigma^+$ state expected to lie increasingly lower than the $^3\Pi_r$ state.

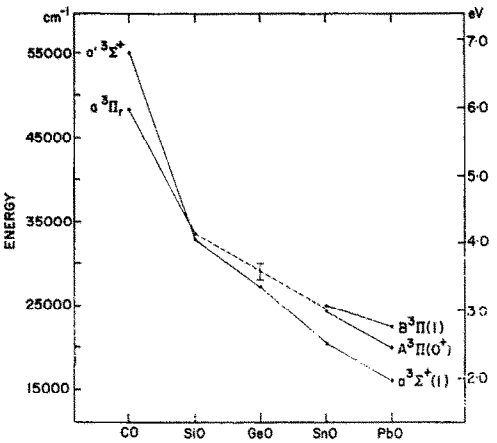

FIG. 7. Comparison of observed T_{00} values for the low-lying excited electronic states of the Group IV oxides. Solid line segments connect states believed to have the same symmetry. The error bars predict the location of the unanalyzed $^3\Pi_r$ state of GeO.

With increasing spin–orbit interaction for the heavier members of the Group IV elements, a Hund's case (*c*) description of the oxides becomes more appropriate. The case (*a*) and case (*c*) states are readily correlated (*21*): The $^1\Sigma^+$ state becomes 0^+; the $^3\Sigma^+$ state becomes 0^- and 1; and the $^3\Pi_r$ state becomes 0^+, 0^-, 1, and 2. In Hund's case (*c*) only the 0^+ and 1 states have electric dipole allowed transitions to the ground state $X\ ^1\Sigma^+(0^+)$.

Since the *a* and *b* states observed in chemiluminescence are the lowest-lying PbO excited states, we identify them as $a\ ^3\Sigma^+(1)$ and $b\ ^3\Sigma^+(0^-)$. The fact that the *a* state radiative lifetime is relatively short compared to the *b* state is in accord with this assignment, namely $a(1) \rightarrow X(0^+)$ is allowed while $b(0^-) \rightarrow X(0^+)$ is formally forbidden. The Ω components of the $^3\Sigma^+$ state are expected to lie close together, as is the case for the *a* and *b* states.

The next-lowest states of PbO are the $A(0^+)$ and the $B(1)$. We assign these states as the $\Omega = 0^+$ and $\Omega = 1$ components of the $^3\Pi_r$ state, as suggested by Barrow, Fry, and Le Bargy (*32*). Since the $\sigma\pi^4\pi^*$ configuration has a lone electron in the π^* molecular orbital, the spin–orbit splitting is expected to be regular, i.e., $E[A\ ^3\Pi(0^+)] < E[B\ ^3\Pi(1)]$. Moreover, this splitting should be relatively large since it arises from the spin–orbit interaction in a $^3\Pi$ state. The observed ordering and separation of the states is in agreement with these predictions. Although the $^3\Pi(0^-)$ state has not been observed, the rotational analysis of the *B*–*X*, *C'*–*X*, and *D*–*X* bands shows perturbations whose forms suggest that they are caused by the $^3\Pi(2)$ state lying above the $B\ ^3\Pi(1)$ state (*12*).

Figure 7 presents a comparative study of the T_{00} values for the lowest-lying electronic states of the diatomic Group IV oxides. Assuming a monotonic trend for the energy levels throughout this homologous series, it should be possible to correlate states of like symmetry. The correspondence between the PbO and CO states determines the end points of this correlation diagram. Figure 7 suggests the location of these states for the intermediate members of this series. Since some information is known about the low-lying states for GeO and SnO, we can reexamine their symmetry assignments.

The only GeO state within the energy region of interest was observed by Hager *et al.* (*30*) in the chemiluminescence from the reaction of germanium vapor with nitrous oxide using a gas-phase flow reactor. A vibrational analysis locates the origin of the state as $T_{00} = 27\,068$ cm^{-1}. Emission from this state has also been observed in matrix-isolation studies by Meyer *et al.* (*33*, *34*) who deduce a gas-phase transition energy of $T_{00} = 26\,900 \pm 200$ cm^{-1} which is in good agreement with the chemiluminescence study. Tewari and Mohan (*35*) found a band system between 460 and 510 nm in the emission from the reaction of germanium vapor with air. They report a value of $T_{00} = 20\,914$ cm^{-1}, but their vibrational analysis is questionable. Their Deslandres scheme appears too diagonal considering that the excited state potential minimum is expected to be at a larger internuclear distance than the ground state. Several of their bandheads appear to coincide with those of Hager *et al.*, and we believe they might be seeing a portion of the same band system.

Apart from the isotope splittings, the head structures of these bands are very similar to those of the SiO $a\ ^3\Sigma^+ \rightarrow X\ ^1\Sigma^+$ transition. This led Hager *et al.* to assign these bands as transitions from the GeO $a\ ^3\Sigma^+$ state. The fact that this is the only state seen in emission from matrix-isolated GeO indicates it is the lowest in the triplet manifold. Therefore, the correlation diagram (Fig. 7) supports the $a\ ^3\Sigma^+(1)$ assignment.

There is some confusion in the literature as to the identification of the lowest-lying excited state of SnO. The emission from a flame containing tin halides or metalic tin was investigated by Joshi and Yamdagni (*36*), who report a $T_{00} = 18\,889$ cm^{-1} for the lowest excited state. Felder and Fontijn (*37*) noted similar bands in the chemiluminescence from the gas-phase reaction of Sn with N_2O, but no reanalysis of the spectrum was attempted. Recently, Linevsky and Carabetta (*38*) analyzed the emission from a $SnCl_4/H_2/N_2O$ flame which is nearly identical to the chemiluminescence spectrum, but located the lowest excited state of SnO at $T_{00} = 20\,437$ cm^{-1}. The positions of many of their bandheads differ by only several angstroms from those seen by Joshi and Yamdagni, and we therefore believe that all the previous investigators saw the same band system. The spectrum of Linevsky and Carabetta is the most extensive and their vibrational numbering is based on the measurement of the isotope shifts for the bandheads, making their analysis the more reliable. Their value is also in reasonably good agreement with the $T_{00} \approx 20\,900$ cm^{-1} reported by Meyer, Smith, and Spitzer (*34*) and Smith and Meyer (*39*) from the emission spectrum of matrix-isolated SnO. Since this is the lowest excited state it should have $^3\Sigma^+(1)$ symmetry. Linevsky and Carabetta found evidence for Q branches on the vibrational bands, as would be expected for the $1 \rightarrow 0^+$ transition to the ground state.

The next two higher states were measured at $T_{00} = 24\,200$ cm^{-1} and $T_{00} = 24\,760$ cm^{-1} in the high-resolution absorption experiments of Deutsch and Barrow (*40*), who identified the symmetries as 0^+ and 1, respectively, and assigned these states as $A\ ^3\Pi(0^+)$ and $B\ ^3\Pi(1)$. The correlation diagram (Fig. 7) supports this assignment.

These two states have also been observed by other workers. The A state has been seen by Joshi and Yamdagni in their flame emission study and they found $T_{00} = 24\,199$ cm^{-1}, in excellent agreement with Deutsch and Barrow. Joshi and Yamdagni also report a second state with $T_{00} = 25\,318$ cm^{-1}, which is probably the B state. The A and B states are also observed in chemiluminescence by Felder and Fontijn and in flame emission by Linevsky and Carabetta, but no T_{00} values are reported in either study.

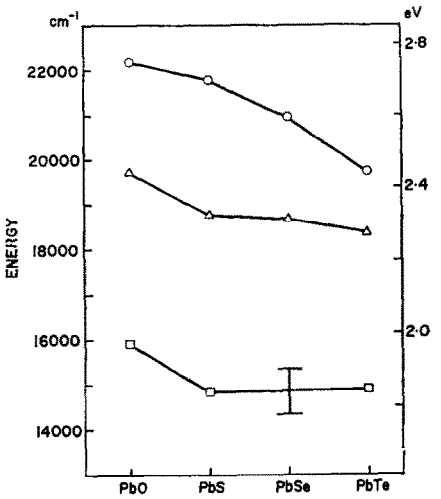

FIG. 8. Comparison of observed T_{00} values for the low-lying excited electronic states of the lead chalconides. Solid line segments connect states believed to have the same symmetry. The circles are for the $B\ ^3\Pi(1)$ state, the triangles are for the $A\ ^3\Pi(0^+)$ state, and the squares are for the $a\ ^3\Sigma^+(1)$ state. The error bars predict the location of the unobserved a state of PbSe. See text for references.

The correlation diagram can be used to predict the location of the yet unanalyzed $^3\Pi_r$ state of GeO. A dashed line is drawn in Fig. 7 connecting the locations of the $^3\Pi_r$ state for SiO and SnO, and we expect the corresponding state of GeO to lie near this line. This places its location at $T_{00} = 29\,000 \pm 1000\ \text{cm}^{-1}$, as indicated in the figure. Sharma and Padur (*41*) observed numerous GeO emission bands between 300 and 500 nm from the reaction of GeH_4 with atomic oxygen. It is not obvious that all these bands arise from the $a\ ^3\Sigma^+ \rightarrow X\ ^1\Sigma^+$ transition, and some may well originate from the $^3\Pi_r$ state.[2]

Similar correlations can also be drawn among the low-lying excited states of the other Group IV chalconides. Figure 8 presents a comparative study of the T_{00} values for the excited states of the lead chalconides. The values for PbS are taken from the extensive gas-phase absorption study of Barrow, Fry, and Le Bargy (*32*). Recently, Teichman and Nixon (*42*) observed emission originating in states with comparable T_{00} values from matrix-isolated PbS upon excitation with an argon/krypton laser. Only sparse information exists for PbSe, and values for this molecule are taken from the early gas-phase absorption study of Walker, Straley, and Smith (*43*). Le Bargy and Barrow (*44*) have analyzed the PbTe a state, while values for the higher-lying PbTe states are from Grove and Ginsburg (*45*).

The correlation is quite straightforward because all the molecules are adequately described by Hund's case (c) coupling. The line segments in Fig. 8 connect states believed to be of the same symmetry. Several important points can be drawn from this figure. First, the correlation of the $a\ ^3\Sigma^+(1)$ state of PbO with the corresponding states

[2] Emission from the GeO $^3\Pi_r$ state has recently been observed in the chemiluminescent reaction of Ge vapor with N_2O by G. A. Capelle and J. M. Brom, Jr. (*J. Chem. Phys.*, to appear). Their analysis locates this state at $T_{00} = 31\,883\ \text{cm}^{-1}$, which is slightly higher than our predicted value.

of PbS and PbTe lends support to our analysis. Second, Fig. 8 predicts the location of the yet-unanalyzed a state of PbSe to be $T_{00} = 14\,850 \pm 500$ cm^{-1}, as indicated in the figure. Barrow (*46*) has informed us that Le Bargy found some weak PbSe absorption bands in the region 6600 to 6950 Å which he thought belonged to a system with $T_{00} \approx 14\,730$ cm^{-1}, in excellent agreement with this prediction. Third, while the locations of the $^3\Pi_r$ and $^3\Sigma^+$ states fall in going from the oxide to the telluride, the decrease is relatively small, which indicates the chalconide atom plays only a minor role in determining the energy of these states. In contrast, Fig. 7 shows a dramatic change in energy of the monoxide states with the identity of the Group IV atom. Finally, Fig. 8 illustrates that the separation of the Ω components of the $^3\Pi_r$ state, i.e., the A and B states, decreases for the lead chalconides in going from oxygen to tellurium. Since this splitting is predominantly caused by the spin–orbit interaction in the lead atom, this implies that the π^* electronic density on this atom decreases through this series of molecules. Meyer, Smith, and Spitzer (*34*) have reached a similar conclusion for the oxides and sulfides of Ge and Sn, namely their extended Hückel calculations show that the π^* density on the metal atom is greater in the oxide than in the corresponding sulfide.

With the assignment of the symmetries of the a, A, and B states of PbO, we are in a position to discuss their different radiative lifetimes. In Hund's case (a), transitions from the $^3\Sigma^+$ and the $^3\Pi_r$ states to the $X\ ^1\Sigma^+$ state can only occur to the extent that other singlet states are mixed into the triplet states (intensity borrowing). As spin–orbit interaction increases, the extent to which these states mix also increases. Thus while the $a\ ^3\Pi_r$ and $a'\ ^3\Sigma^+$ states of CO have extremely long lifetimes, the radiative lifetimes for the corresponding states in PbO are considerably shortened. Although gas-phase radiative lifetimes have not been measured for SiO, GeO, and SnO, the A state radiative lifetime can be inferred from matrix-isolation lifetime studies. Meyer *et al.* (*34*) estimate for the A states of SiO, GeO, and SnO the lifetimes 48, 2.0, and 0.33 msec, respectively. Our gas-phase lifetime value of 3.75 μsec for the PbO A state and 2.58 μsec for the PbO B state follows the expected trend to shorter lifetimes.

From first-order perturbation theory, the transition probability (and therefore the reciprocal of the radiative lifetime) is proportional to two factors: (i) the square of the spin–orbit matrix element connecting the triplet to the singlet state with oscillator strength; and (ii) the inverse square of energy difference between the interacting states. The lowest-lying excited state with a fully allowed electric dipole transition to the ground state is the PbO $D\ ^1\Pi(1)$ state at $T_{00} = 30\,100$ cm^{-1}. It is presumably the interaction with this state which causes the lifetime shortening. It is interesting to note that if we assume that the first factor, namely the square of the spin–orbit matrix elements, is the same for both triplet states, then the difference in the square of the energy separations predicts $\tau(a)$ is roughly three times longer than $\tau(B)$. Although we were unable to measure $\tau(a)$, we established that $\tau(a) \geq 10$ μsec. Considering the crudeness of this approximation, this is consistent with the above argument and our value for $\tau(B)$.

Finally, we speculate on how the radiative lifetime changes in going from oxygen to tellurium for a given lead chalconide excited state. As remarked previously, the π^* electron density on the lead atom decreases with increasing mass of the chalconide atom. Since it is the spin–orbit mixing with the $D\ ^1\Pi(1)$ state, caused primarily by the metal atom, that shortens the radiative lifetime, we expect the radiative lifetime of the corresponding excited state to lengthen in going from the oxide to the telluride (reversal of

the heavy atom effect). Although unfortunately there appears to be no information on the radiative lifetimes of the other lead chalconides so that we can test this prediction, Meyer *et al.* (*34*) have observed longer A state radiative lifetimes for SnS compared to SnO and GeS compared to GeO, which they have attributed to this π^* electron density trend.

ACKNOWLEDGMENTS

We warmly thank R. F. Barrow for helpful correspondence and S. G. Hadley for useful discussions. Support from the Army Research Office (Durham) under DA-ARO-D-31-124-73-G147 for the chemiluminescence studies and from the Air Force Office of Scientific Research under AFOSR-73-2551A for the lifetime studies is gratefully acknowledged.

RECEIVED: May 15, 1975

REFERENCES

1. S. N. SUCHARD, "Spectroscopic Constants for Selected Heteronuclear Diatomic Molecules," Vols. I, II, III, Wiley, New York, to be published.
2. J. RAFERTY, R. P. SCOTT, AND W. G. RICHARDS, *J. Phys. B* **5**, 1293 (1972); P. R. SCOTT, J. RAFERTY, AND W. G. RICHARDS, *J. Phys. B* **6**, 881 (1973).
3. P. H. KRUPENIE, "The Band Spectrum of Carbon Monoxide," NSRDS-NBS 5, U. S. Government Printing Office, Washington, D. C., 1966.
4. R. F. BARROW, *Proc. Phys. Soc.* **56**, 204 (1944).
5. H. LAMPRECHT, *Z. Wiss. Photog. Photoph. Photochem.* **33**, 10, 16 (1911).
6. J. M. EDER AND E. VALENTA, *Atlas Typischer Spectren* **17**, (1924).
7. L. GREBE AND H. KONEN, *Phys. Z.* **22**, 546 (1921).
8. S. BLOOMENTHAL, *Phys. Rev.* **35**, 34 (1930).
9. E. N. SHAWHAN AND F. MORGAN, *Phys. Rev.* **47**, 377 (1935).
10. H. G. HOWELL, *Proc. Roy. Soc. Longon Ser. A* **153**, 683 (1935).
11. E. E. VAGO AND R. F. BARROW, *Proc. Phys. Soc.* **59**, 44 (1947).
12. R. F. BARROW, J. L. DEUTSCH, AND D. N. TRAVIS, *Nature* **191**, 374 (1961).
13. A. CHRISTY AND S. BLOOMENTHAL, *Phys. Rev.* **35**, 46 (1930).
14. R. S. RAM, J. SINGH, AND K. N. UPADHYA, *Spectrosc. Lett.* **6**, 515 (1973).
15. R. C. OLDENBORG, J. L. GOLE, AND R. N. ZARE, *J. Chem. Phys.* **60**, 4032 (1974).
16. R. N. ZARE AND P. J. DAGDIGIAN, *Science* **185**, 739 (1974).
17. C. R. DICKSON AND R. N. ZARE, *Chem. Phys.* **7**, 361 (1975).
18. R. C. OLDENBORG, Ph.D. Thesis, Columbia University, 1975.
19. AN. N. NESMEYANOV, "Vapor Pressure of the Elements," Academic Press, New York, 1963.
20. C. R. DICKSON AND R. N. ZARE, to be published.
21. G. HERZBERG, "Spectra of Diatomic Molecules," Van Nostrand Reinhold, New York, 1960.
22. P. J. DAGDIGIAN, H. W. CRUSE, AND R. N. ZARE, *J. Chem. Phys.* **62**, 1824 (1975).
23. S. E. JOHNSON, Ph.D. Thesis, University of California, Santa Barbara, 1971.
24. D. GOLOMB AND G. T. BEST, "Photoluminescence of PbO in the Upper Atmosphere," *Trans. AGU* **55**, 366 (1974).
25. J. DROWART, R. COLIN, AND G. EXSTEEN, *Trans. Faraday Soc.* **61**, 1293 (1965).
26. J. L. GOLE AND R. N. ZARE, *J. Chem. Phys.* **57**, 5331 (1972).
27. M. YOSHIMINE AND A. D. MCLEAN, *Int. J. Quantum Chem.* **1S**, 313 (1967).
28. W. M. HUO, *J. Chem. Phys.* **43**, 624 (1965).
29. J. W. RAYMONDA, J. S. MUENTER, AND W. A. KLEMPERER, *J. Chem. Phys.* **52**, 3458 (1970), and references therein.
30. G. HAGER, L. E. WILSON, AND S. G. HADLEY, *Chem. Phys. Lett.* **27**, 439 (1974); G. HAGER, R. HARRIS, AND S. G. HADLEY, *J. Chem. Phys.*, to be published.
31. H. BREDOHL, R. CORNET, I. DUBOIS, AND F. REMY, *J. Phys. B: Atom. Mol. Phys.* **7**, L66 (1974).
32. R. F. BARROW, P. W. FRY, AND R. C. LE BARGY, *Proc. Phys. Soc.* **81**, 697 (1963).

33. B. MEYER, Y. JONES, J. J. SMITH, AND J. SPITZER, *J. Mol. Spectrosc.* **37**, 100 (1971).
34. B. MEYER, J. J. SMITH, AND K. SPITZER, *J. Chem. Phys.* **53**, 3616 (1970).
35. D. P. TEWARI AND H. MOHAN, *J. Mol. Spectrosc.* **39**, 290 (1971).
36. M. M. JOSHI AND R. YAMDAGNI, *Indian J. Phys.* **41**, 275 (1967).
37. W. FELDER AND A. FONTIJN, *Chem. Phys. Lett.*, to be published.
38. M. J. LINEVSKY AND R. Z. CARABETTA, unpublished results.
39. J. J. SMITH AND B. MEYER, *J. Mol. Spectrosc.* **27**, 304 (1968).
40. E. W. DEUTSCH AND R. F. BARROW, *Nature* **201**, 815 (1964).
41. A. SHARMA AND J. P. PADUR, *Proc. Phys. Soc.* **90**, 269 (1967).
42. R. A. TEICHMAN III AND E. R. NIXON, *J. Mol. Spectrosc.* **54**, 78 (1975); **55**, 192 (1975)
43. J. W. WALKER, J. W. STRALEY, AND A. W. SMITH, *Phys. Rev.* **53**, 140 (1938).
44. R. C. LE BARGY AND R. F. BARROW, *Proc. Phys. Soc.* **82**, 332 (1963).
45. R. GROVE AND N. GINSBURG, *Spectrochim. Acta* **16**, 730 (1960).
46. R. F. BARROW, private communication.